american physiological society
AMERICAN JOURNAL OF PHYSIOLOGY
RENAL PHYSIOLOGY

Am J Physiol Renal Physiol 321: F000–F000, 2021.
First published October 4, 2021; doi:10.1152/ajprenal.00207.2021

RESEARCH ARTICLE

Expression of claudin-8 is induced by aldosterone in renal collecting duct principal cells

AQ:1-4

AQ: au

Ali Sassi,[1,2*] Yubao Wang,[1,2*] Alexandra Chassot,[1,2] Isabelle Roth,[1] Suresh Ramakrishnan,[1,2] Valérie Olivier,[1,2] Olivier Staub,[3] Khalil Udwan,[1] and Eric Feraille[1,2]

[1]*Department of Cellular Physiology and Metabolism, University of Geneva, Geneva, Switzerland;* [2]*National Center of Competence in Research "Kidney.ch," Switzerland; and* [3]*Department of Biomedical Sciences, University of Lausanne, Lausanne, Switzerland*

AQ: 5

Abstract

Fine tuning of Na^+ reabsorption takes place along the aldosterone-sensitive distal nephron, which includes the collecting duct (CD), where it is mainly regulated by aldosterone. In the CD, Na^+ reabsorption is mediated by the epithelial Na^+ channel and Na^+ pump (Na^+-K^+-ATPase). Paracellular ion permeability is mainly dependent on tight junction permeability. Claudin-8 is one of the main tight junction proteins expressed along the aldosterone-sensitive distal nephron. We have previously shown a coupling between transcellular Na^+ reabsorption and paracellular Na^+ barrier. We hypothesized that aldosterone controls the expression levels of both transcellular Na^+ transporters and paracellular claudin-8 in a coordinated manner. Here, we show that aldosterone increased mRNA and protein levels as well as lateral membrane localization of claudin-8 in cultured CD principal cells. The increase in claudin-8 mRNA levels in response to aldosterone was prevented by preincubation with 17-hydroxyprogesterone, a mineralocorticoid receptor antagonist, and by inhibition of transcription with actinomycin D. We also showed that a low-salt diet, which stimulated aldosterone secretion, was associated with increased claudin-8 abundance in the mouse kidney. Reciprocally, mice subjected to a high-salt diet, which inhibits aldosterone secretion, or treated with spironolactone, a mineralocorticoid receptor antagonist, displayed decreased claudin-8 expression. Inhibition of glycogen synthase kinase-3, Lyn, and Abl signaling pathways prevented the effect of aldosterone on claudin-8 mRNA and protein abundance, suggesting that signaling of protein kinases plays a permissive role on the transcriptional activity of the mineralocorticoid receptor. This study shows that signaling via multiple protein kinases working in concert mediates aldosterone-induced claudin-8 expression in the CD.

NEW & NOTEWORTHY In this study, we showed that aldosterone modulates claudin-8 expression in cultured collecting duct principal cells and in the mouse kidney. The upregulation of claudin-8 expression in response to aldosterone is dependent on at least glycogen synthase kinase-3, Lyn, and Abl signaling pathways, indicating the participation of multiple protein kinases to the effect of aldosterone.

aldosterone; claudin; collecting duct; kidney; sodium transport

INTRODUCTION

The regulation of Na^+ transport by the kidneys is crucial for the maintenance of body fluid homeostasis and blood pressure control. The collecting duct (CD) plays a major role in controlling Na^+ balance. In this segment, Na^+ reabsorption is mainly achieved by the apical epithelial Na^+ channel (ENaC) and basolateral Na^+ pump (Na^+-K^+-ATPase), which provides the electrochemical gradient for vectorial transcellular Na^+ transport. The CD is characterized by a tight epithelium displaying an interconnected network of tight junctions, resulting in a strict separation of luminal and interstitial spaces. The main function of tight junctions in the CD is to prevent paracellular backflow of water and solutes, especially Na^+, to the tubular lumen. Claudins are major structural components of tight junctions that determine the paracellular permeability to water and solutes. The expression profile of claudins in the kidney tubule is segment specific, and they can generate either a diffusion barrier or a paracellular permeability pathway (1). Claudin-8 is highly expressed in the CD (1–3), where it has been described to play a major role in Na^+ barrier formation together with Cl^- permeability and has been implicated in the generation of high electrical resistance (1, 4, 5). We recently showed that the ENaC γ-subunit determines claudin-8 abundance, suggesting a coupling between paracellular and transcellular Na^+ permeability (5).

Aldosterone is the main hormonal stimulus of Na^+ reabsorption by the CD. Aldosterone binding to the mineralocorticoid receptor (MR) induces its nuclear translocation and

* A. Sassi and Y. Wang contributed equally to this work.

AQ: 6 Correspondence: E. Feraille (Eric.Feraille@unige.ch).

Submitted 1 June 2021 / Revised 28 September 2021 / Accepted 28 September 2021

AQ: 7 the transcription of specific genes (6). Aldosterone first induces early genes, such as serum/glucocorticoid-regulated kinase 1 (Sgk-1) and GILZ, that increase ENaC open probability AQ: 8 and decrease its internalization and degradation (7–9). Aldosterone also rapidly increases cell-surface expression of active Na^+-K^+-ATPase units (10). Increased expression levels of α-ENaC and Na^+-K^+-ATPase α- and β-subunits in response to long-term aldosterone stimulation upregulate the Na^+ reabsorption capacity of principal cells (10). Cell-specific expression of 11β-hydroxysteroid dehydrogenase type 2, which prevents MR occupancy by glucocorticoids, confers aldosterone responsiveness (11). Na^+ transport by principal cells is also modulated by hormonal factors such as vasopressin, angiotensin II, or insulin and paracrine/autocrine factors such as endothelin-1 and eicosanoids (10, 12–14).

Aldosterone-induced transcellular Na^+ reabsorption generates a negative transepithelial potential that, combined with the interstitial-to-lumen Na^+ gradient, may lead to paracellular backflow of reabsorbed Na^+. Indeed, microperfused mouse cortical CDs secrete Na^+ under a physiological basal-to-apical Na^+ concentration gradient (15). The efficiency of Na^+ reabsorption may be compromised by increased paracellular Na^+ backflow. Interestingly, reduced paracellular Na^+ permeability associated with increased claudin-8 expression levels in response to aldosterone has been shown in the human colon (16). However, the control of tight junction composition by aldosterone remains to be established along the kidney tubule.

In this study, we showed that aldosterone increases claudin-8 abundance in CD principal cells. We also showed that upregulation of claudin-8 expression in response to aldosterone is dependent on at least glycogen synthase kinase-3 (GSK3), Lyn, and Abl signaling pathways. Taken together, these results reveal a new mechanism of hormonal modulation of the junctional complex via the upregulation of claudin-8 expression by multiple protein kinases.

METHODS

Cell Culture and Electrical Measurements

$mCCD_{cl1}$ cells were grown on permeable filters (Transwell, Corning Costar, Cambridge, MA) as previously described (17). The potential difference and transepithelial resistance were measured using a Millicell-ERS Volt-Ohm meter (Millipore, Billerica, MA). γ-ENaC-TetOn-mCCD cells overexpressing the ENaC γ-subunit in a doxycycline-inducible manner (17) were cultured in the presence or absence of doxycycline (Dox; 1.25 μg/mL). Aldosterone (10^{-6} M) and inhibitors of lysosomal protein degradation and aldosterone-activated kinases were added to the apical and basal compartments 24 h before cell lysis.

Retrovirus Production and Cell Transduction

For gene overexpression, wild-type green fluorescence protein (GFP) and wild-type mouse α-ENaC cDNAs were subcloned into a modified pSF-lenti vector (Sigma) resistant to puromycin. pSF-lenti was transiently transfected in packaging HEK293T cells using a Polyplus-transfection jetPRIME kit according to the manufacturer's instructions. Lentiviral particles were collected after 72 h, and γ-ENaCTetOn-mCCD cells were transduced. Stable cell lines were obtained after puromycin selection (2 μg/mL). Claudin-8 gene silencing was performed as previously described (5).

RNA Extraction and RT-PCR

RNA extraction and real-time PCR were performed as previously described (5). The primers used for PCR are shown in Table 1. T1

Western Blot Analysis

Equal amounts of protein from cultured cells or the kidney cortex were separated by 4–20% SDS-PAGE (Witec) and transferred to polyvinylidene difluoride membranes (Immobilion-P, Millipore) as previously described (17). After incubation with primary antibodies (Table 2), membranes were incubated T2 with anti-rabbit or anti-mouse IgG antibody coupled to horseradish peroxidase (Transduction Laboratories, Lexington, KY). The antigen-antibody complexes were detected by enhanced chemiluminescence (Advansta, Menlo Park, CA). Protein abundance was quantified with ImageJ software. Results are expressed as the ratio of the densitometry of the band of interest to the loading control.

Immunofluorescence

Cells grown to confluence on polycarbonate filters were fixed (together with filters) with ice-cold methanol for 5 min at −20°C and then washed with PBS. After samples had been washed for 30 min, blockade of nonspecific binding sites was done with PBS containing 2% BSA (PBS-BSA) at room

Table 1. *Sequences of primers used for real-time PCR*

Name	Forward	Reverse
P0	5′-AATCTCCAGAGGCACCATTG-3′	5′-GTTCAGCATGTTCAGCAGTG-3′
Claudin-4	5′-AAGTGCACCAACTGCATGGA-3′	5′-GGCTCCGGCGGTGATC-3′
Claudin-7	5′-AAGCGAAGAAGGCCCGAATA-3′	5′-GCAAGACCTGCCACAATGAA-3′
Claudin-8	5′-GTGCTGCGTCCGTCTTGGCT-3′	5′-TCGTCCCCCGTGCATCTGGT-3′
ZO-1	5′-TTATGCGCAGTGGTATCCAATT-3′	5′-TCCGGACACAACCTCATCCT-3′
Sgk-1	5′-CCAAACCCTCCGACTTTCAC-3′	5′-CCTTGTGCCTAGCCAGAAGAA-3′
α-ENaC	5′-CAGACTTGGAGCTTTGACAAGGA-3′	5′-ACTTCTCTGTGCCTTGTTTATATGTGTT-3′
γ-ENaC	5′-CCGAGATCGAGACAGCAATGT-3′	5′-CGCTCAGCTTGAAGGATTCTG-3′
Abl	5′-CAGTGAAAATGACCCCAACC-3′	5′-GTTTGGGCTTCACACCATTC-3′
GSK-3	5′-CGCTTCCCTTCTTCATTGAC-3′	5′-ACGTGAACGAGGGCAAATAC-3′
Lyn	5′-ATCAACTTCGGCTGCTTCAC-3′	5′-CATCACATCTGCGTTGGTTC-3′

EnaC, epithelial Na^+ channel; GSK3, glycogen synthase kinase-3; Sgk-1, serum/glucocorticoid-regulated kinase 1; ZO-1, zonula occludens-1.

Table 2. *Antibodies used for Western blots*

Name	Species	Dilution	Supplier	Cat. No.
Claudin-4	Mouse	1/500	ThermoFisher (Waltham, MA)	32-9400
Claudin-7	Rabbit	1/500	ThermoFisher	34-9100
Claudin-8	Rabbit	1/500	ThermoFisher	40-0700Z
ZO-1	Rabbit	1/1,000	ThermoFisher	61-7300
Sgk-1	Rabbit	1/1,000	Sigma-Aldrich (St. Louis, MO)	S5188
α-ENaC	Rabbit	1/1,000	Prof. J. Loffing (University of Zürich, Zurich, Switzerland) (18)	
γ-ENaC	Rabbit	1/500	StressMarq (Victoria, BC, Canada)	SPC-405
β-actin	Mouse	1/10,000	Sigma-Aldrich	A5441
E-cadherin	Mouse	1/5,000	BD Biosciences (Franklin Lakes, NJ)	610181

EnaC, epithelial Na^+ channel; Sgk-1, serum/glucocorticoid-regulated kinase 1; ZO-1, zonula occludens-1

temperature. Finally, cells were incubated overnight at 4°C with antibodies against claudin-8 and Sgk-1 diluted 1:500 in 0.2% PBS-BSA followed by 1 h of incubation with Alexa Fluor 488-conjugated goat anti-rabbit (Cat. No. A-11017, Invitrogen) diluted 1:500 in PBS-BSA. Samples were mounted on microscope slides using Vectashield mounting medium (Maravai Life Science, San Diego, CA) with DAPI for nuclear counterstaining. Fluorescence images were acquired using a LSM 700 confocal laser scanning microscope (Carl Zeiss, Oberkochen, Germany) using 488-nm ray lasers. The distance between the *Z*-slices was 0.25 μm. Five to ten *Z*-stack images were processed using ZEISS ZEN imaging software (ZEN 2.3, Carl Zeiss).

Tyrosine Kinase Activity Profiling

A Pamchip array was used to analyze the effect of the aldosterone on protein kinase activity (Pamgene, Hertogenbosch, The Netherlands). The Pamchip contains 136 phosphorylation sites of 144 peptides each consisting of 12–15 amino acids, with one or more phosphorylation sites. We used two different types of arrays with peptides containing tyrosine or serine/threonine phosphorylation sites. $mCCD_{cl1}$ cells were grown and stimulated or not with 10^{-6} M aldosterone for 24 h. Cells were harvested and lysed for 15 min at 4°C with Mammalian Protein Extraction Reagent (Pamgene) and phosphatase and protease inhibitors (Thermo Scientific). Next, lysates were centrifuged at 16,000 *g* for 15 min at 4°C, and 40 μL of sample mix was subsequently prepared using reaction buffer (1× PK buffer), fluorescent-labeled antibody (Pamgene), 400 μM ATP, 10 mM dithiothreitol, and 7.5 μg of lysate protein. The arrays were blocked using 2% BSA for 30 min, and the sample mix was loaded. Analysis was done using a Pamstation 96 instrument (Pamgene). Spot intensity was corrected for local background, and initial phosphorylation rates were calculated using BioNavigator software (Pamgene).

Animals

Male C57B6 mice (Charles River, Saint Germain de l'Arbresle, France) were fed for 7 days with either low-Na^+ diet [0.01% (wt/wt); LSD], normal-Na^+ diet [0.18% (wt/wt); NSD], or high-Na^+ diet [1.25% (wt/wt); HSD] (Provimi-Kliba, Kaiseraugst, Switzerland). One group of mice that were fed the low-Na^+ diet received 0.35 mg/100 g body wt/day of spironolactone mixed with food for 7 days. Animals had free access to food and water. Kidney tubule-specific Sgk-1 knockout mice have been previously described (19). The veterinary local ethical committee of animal care of Geneva approved all animal experiments.

Statistics

Results are expressed as means ± SD from several experiments. Statistical differences were analyzed using GraphPad Prism software. Student's *t* test or one-way ANOVA was used for comparisons between two groups or more than two groups, respectively.

RESULTS

Aldosterone Increases Expression of Claudin-8 in Cultured Mouse CD Principal Cells

We assessed the effect of aldosterone in the regulation of expression levels of tight junction core proteins in the CD. In $mCCD_{cl1}$ cells, a model of CD principal cells (18), aldosterone treatment increased transepithelial current but did not significantly alter the transepithelial resistance (Fig. 1*A*). ENaC blockade by the addition of 10^{-5} M benzamil to the apical side of the cell monolayer only slightly increased the transepithelial resistance in both control and aldosterone-treated cells (Supplemental Fig. S1; all Supplemental material is available at https://doi.org/10.6084/m9.figshare.16652182.v1.), indicating that variations of ENaC activity only modestly alter transepithelial resistance. We then assessed the effect of aldosterone on the main claudin species expressed in the CD, that is , claudin-4, claudin-7, and claudin-8. We consistently showed that aldosterone treatment was associated with increased protein expression levels of Sgk-1, a classical aldosterone-induced gene (Fig. 1*B*). Claudin-8 protein abundance was increased in response to aldosterone, but the abundance of claudin-4, claudin-7, and zonula occludens-1, a tight junction-associated protein, was unchanged (Fig. 1*B*). The effect of aldosterone on Sgk-1 and claudin-8 was confirmed by immunofluorescence imaging, as shown in Fig. 1*C*. The results showed that claudin-8 immunoreactivity detected along the lateral membrane increased in response to aldosterone (Fig. 1*C*, *bottom*). The aldosterone effect on claudin-8 expression levels was also observed at the mRNA level, as shown in Fig. 1*D*.

These results indicate that claudin-8 expression is specifically induced by aldosterone in cultured mouse CD principal cells.

Aldosterone Modulates Claudin-8 Expression in a Dose- and Time-Dependent Manner in Cultured Mouse CD Principal Cells

To determine the amount of aldosterone necessary to produce an increase in claudin-8 abundance, cells were incubated

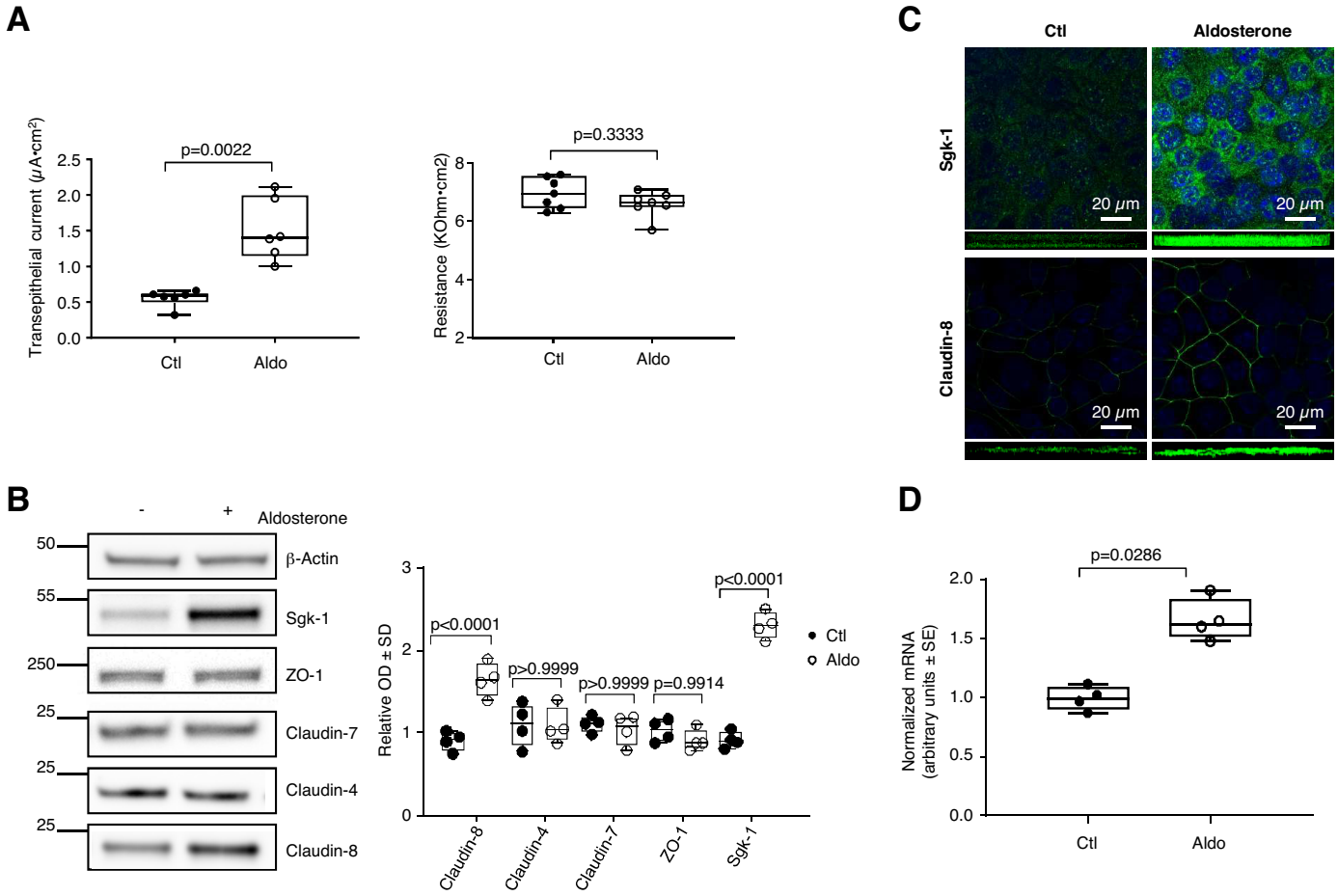

COLOR

Figure 1. Aldosterone (Aldo) modulates the expression of claudin-8 in cultured mouse collecting duct principal cells. $mCCD_{cl1}$ cells were grown to confluence on filters and treated or not treated with 10^{-6} M aldosterone for 24 h. *A*: measured transepithelial resistance (TER; *right*, lumen negative) and calculated transepithelial currents (I_{sc}; *left*). *B*: representative immunoblots showing the effect of aldosterone treatment on claudin-4, claudin-7, claudin-8, serum/glucocorticoid-regulated kinase 1 (Sgk-1), and zonula occludens-1 (ZO-1) protein abundance. β-Actin was used as a loading control (*left*). The right graph shows the relative densitometric quantification of immunoblots from 4 independent experiments. *C*: immunofluorescence staining of claudin-8 and Sgk-1 in confluent monolayers treated or not treated with 10^{-6} M aldosterone for 24 h. The *bottom* part of each image is an optical section obtained from the *Z*-stack. *D*: claudin-8 mRNA levels as assessed by real-time PCR. Results are means ± SD from 4 independent experiments. Statistical analysis was performed by a Kruskal–Wallis test (*A*) and one-way ANOVA (*B*). Ctl, control; OD, optical density.

with increasing concentrations of aldosterone (10^{-10} to 10^{-6} M) for 24 h. As shown in Fig. 2*A*, 10^{-9} and 10^{-8} aldosterone induced a small but nonsignificant increase in claudin-8 protein abundance followed by a larger and significant increase in claudin-8 protein abundance at 10^{-7} M and 10^{-6} M (Fig. 2*A*). We next investigated the time course effect of aldosterone. Cells were incubated in media containing aldosterone (10^{-6} M) for variable periods of time (3, 6, 12, 24, and 36 h). After a lag time, claudin-8 protein was progressively induced in a time-dependent manner by aldosterone, with a maximal effect observed after 24 h and sustained after 36 h (Fig. 2*B*). These results indicate that aldosterone modulates claudin-8 expression in a dose- and time-dependent manner in cultured mouse CD principal cells. The transepithelial potential difference also progressively increased in a time-dependent manner by aldosterone (Fig. 2*C*). However, the time courses of changes in transepithelial potential and claudin-8 expression were different, suggesting that claudin-8 is not induced via changes in transepithelial ion transport. This finding is in agreement with our previous report showing that transepithelial potential and Na^+ transport are not involved in the modulation of claudin-8 expression (5).

We then assessed whether aldosterone modulates claudin-8 abundance via the MR. For this purpose, $mCCD_{cl1}$ cells were preincubated for 1 h with 10^{-5} M 17-hydroxyprogesterone, an MR antagonist (20), before the addition of 10^{-6} M aldosterone for 24 h. The results showed that 17-hydroxyprogesterone blunted the induction of both Sgk-1 and claudin-8 by aldosterone (Fig. 2*D*), suggesting that these effects of aldosterone are mediated via the MR.

Increased Claudin-8 Expression in Response to Aldosterone Relies on Increased Transcription in Cultured Mouse CD Principal Cells

To assess whether increased claudin-8 abundance in response to aldosterone relies on transcription, $mCCD_{cl1}$ cells were incubated in the presence of 10^{-6} M actinomycin D with or without 10^{-6} M aldosterone for 24 h. The results showed that actinomycin D prevented the aldosterone-induced increase in both Sgk-1 and claudin-8 mRNA and

J_ID: AJPRENAL ART NO: F-00207-2021 Date: 11-October-21 12:00 Page: 5 Total Pages: 13 ini: 6//RM

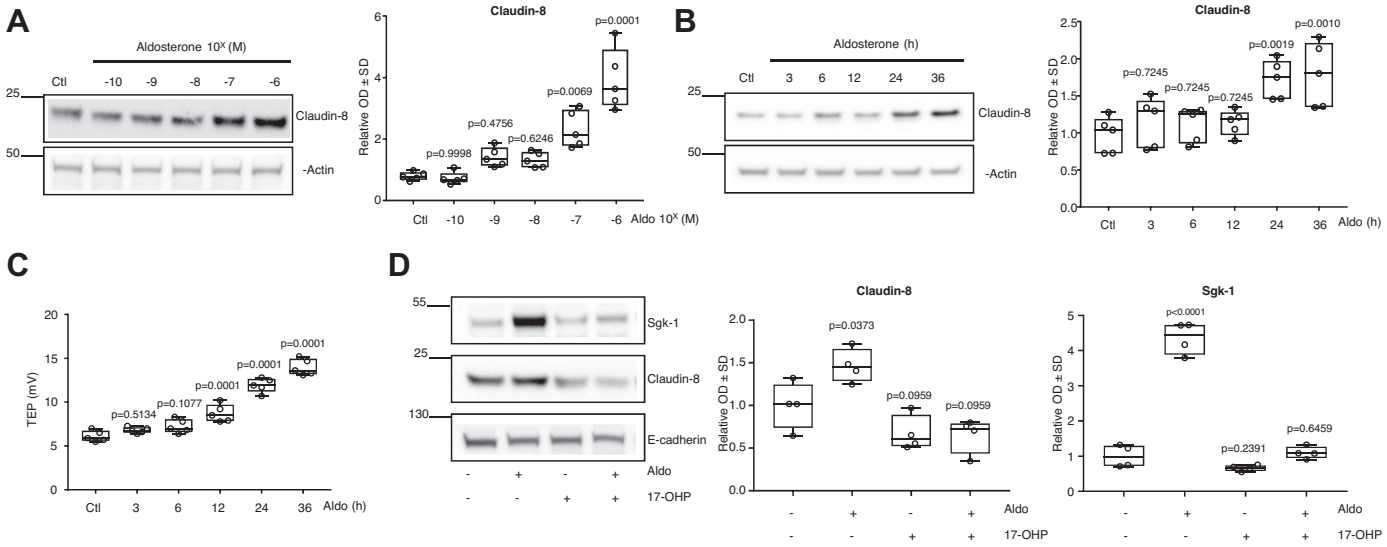

Figure 2. Aldosterone (Aldo) modulates claudin-8 expression in a dose- and time-dependent manner in cultured mouse collecting duct principal cells. $mCCD_{cl1}$ cells were grown to confluence on filters and treated or not treated with variable concentrations of aldosterone (10^{-10} to 10^{-6} M) for 24 h (*A*); or treated or not treated with 10^{-6} M aldosterone for various periods of time (3, 6, 12, 24, and 36 h) (*B*); and preincubated or not preincubated for 1 h with 10^{-5} M 17-hydroxyprogesterone (17-OHP) (*D*). *A*, *left*: representative immunoblots showing the dose dependence of aldosterone treatment on claudin-8 abundance. *Right*, graph depicting the relative densitometric quantification of immunoblots from 5 independent experiments. *B*, *left*: representative immunoblots showing the time course of aldosterone treatment on claudin-8. *Right*, graph depicting relative densitometric quantification of immunoblots from 5 independent experiments. β-Actin was used as a loading control. *C*: measured transepithelial potential difference (TEP). *D*, *left*: representative immunoblots showing the effect of 17-OHP and aldosterone treatment on claudin-8 abundance. *Right*, graphs depicting the relative densitometric quantification of immunoblots from 4 independent experiments. E-cadherin was used as a loading control. Results are means ± SD from at least 4 independent experiments. Statistical analysis was performed by one-way ANOVA. Ctl, control; OD, optical density; Sgk-1, serum/glucocorticoid-regulated kinase 1.

F3 protein levels (Fig. 3, *A* and *B*), suggesting that increased transcription is the main mechanism accounting for the effect of aldosterone. This interpretation was strengthened by in silico analysis (The Eukaryotic Promoter Database, available online at https://epd.epfl.ch) of the mouse claudin-8 promoter, which displays several glucocorticoid receptor (GR)- and MR-binding sites (Fig. 3*C*, *bottom*). In silico analysis of the promoter of mouse Sgk-1, a well-

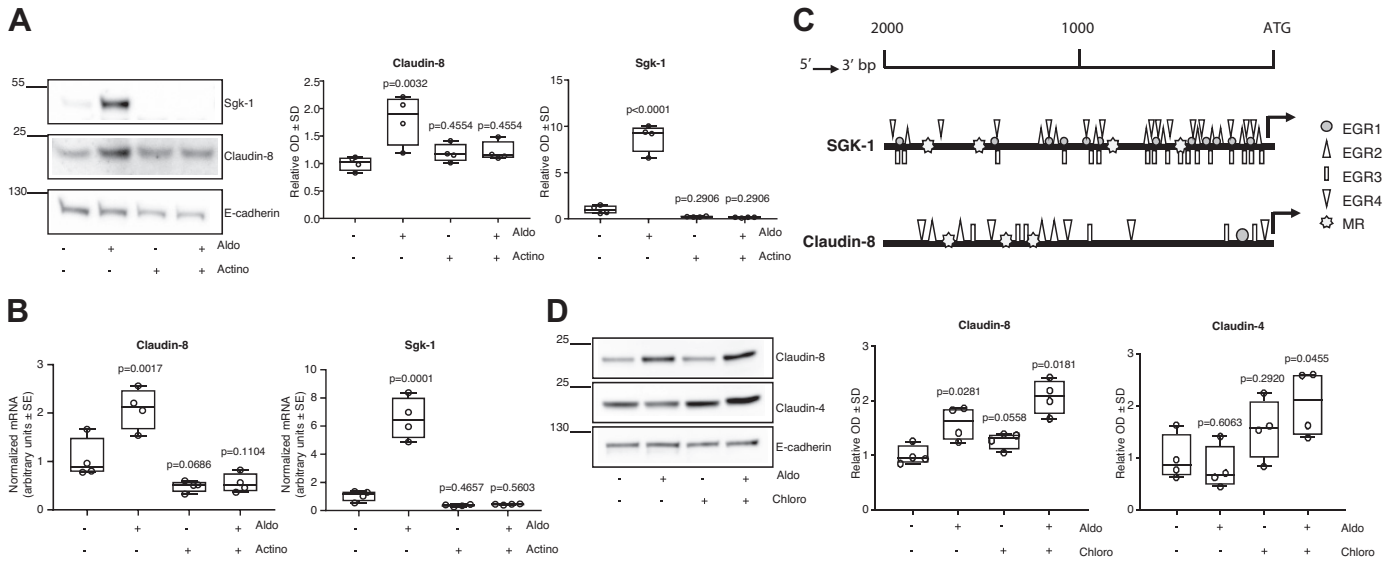

Figure 3. Effect of aldosterone (Aldo) on protein degradation of claudin-8 in cultured mouse collecting duct principal cells. $mCCD_{cl1}$ cells were grown to confluence on filters and treated or not treated with 10^{-6} M aldosterone and/or 10^{-6} M actinomycin D (Actino; *A*) and/or 10^{-5} M chloroquine (Chloro; *D*) for 24 h. *A*, *left*: representative immunoblots showing the effect of aldosterone and/or actinomycin D treatment on claudin-8 and serum/glucocorticoid-regulated kinase 1 (Sgk-1). *Right*, graphs depicting relative densitometric quantification of immunoblots from 4 experiments. *B*: claudin-8 (*left*) and Sgk-1 (*right*) mRNA levels as assessed by real-time PCR. *C*: diagrams of the putative promoter region (2 kb) of mouse Sgk-1 and claudin-8 genes. Diagrams show epidermal growth factor receptor (EGFR) and mineralocorticoid receptor (MR) transcription factor binding sites. Putative sites were predicted in the Eukaryotic Promoter Database (available online at https://epd.epfl.ch). *D*, *left*: representative immunoblots showing the effect of aldosterone and/or chloroquine treatment on claudin-8 and claudin-4 abundance. *Right*, graphs depicting relative densitometric quantification of immunoblots from 4 experiments. E-cadherin was used as a loading control. Statistical analysis was performed by one-way ANOVA. OD, optical density.

AQ: 18

characterized aldosterone-induced gene, is given for comparison (Fig. 3*C*, *top*).

We next assessed the possibility of additional posttranscriptional control of claudin-8 expression via inhibition of protein degradation by aldosterone. We assessed the effect of chloroquine, an inhibitor of lysosomal protein degradation, the major pathway of transmembrane protein degradation. Figure 3*D* shows that inhibition of lysosomal protein degradation slightly but not significantly increased claudin-8 abundance but did not alter the amplitude of the effect of aldosterone on claudin-8 protein expression. However, increased abundance of claudin-4 protein was associated with chloroquine treatment (Fig. 3*D*), indicating that chloroquine was active. These results suggest that claudin-8 protein is most likely slowly degraded via the lysosomal pathway and that its degradation is not regulated by aldosterone.

The increase in claudin-8 protein abundance in response to aldosterone was abolished in cells stably transduced with an shRNA specifically targeting claudin-8 (Supplemental Fig. S2). This observation further supports that the effect of aldosterone mostly if not exclusively relies on increased claudin-8 transcription.

Aldosterone Increases Claudin-8 Expression in the Mouse Kidney

Further examining the potential physiological effect of aldosterone on claudin-8 in vivo, we compared its protein expression level in mice fed with an NSD with that in mice fed with an LSD or HSD. Compared with the NSD, 7 days of the LSD increased the expression level of the aldosterone-induced genes Sgk-1 and α-ENaC in the kidney cortex, whereas the opposite changes were observed in mice fed with the HSD (Fig. 4*A*). These results indicate that the LSD increased endogenous aldosterone, whereas the HSD did the opposite. Claudin-8 protein was more abundant in the kidneys of mice fed with the LSD. Opposite changes were seen in mice fed with the HSD (Fig. 4*A*). These changes in claudin-8 protein abundance were not associated with parallel changes in claudin-8 mRNA levels (Supplemental Fig. S3).

To confirm the role of aldosterone in the control of claudin-8 expression level, mice that were fed the LSD were treated for 7 days with spironolactone, an MR antagonist. Spironolactone decreased α-ENaC expression levels, indicating that aldosterone effects were effectively antagonized (Fig. 4*B*). The claudin-8 expression level was also decreased by spironolactone (Fig. 4*B*). These results confirmed our in vitro results and indicated that endogenous aldosterone variation is associated with parallel changes in claudin-8 abundance.

Role of α-ENaC and Sgk-1 in Changes of Claudin-8 Expression Levels in Response to Aldosterone

We investigated whether the effect of aldosterone on claudin-8 abundance relied on increased α-ENaC expression. Indeed, aldosterone stimulates Na^+ reabsorption in the CD by increasing the activity of ENaC by inducing expression levels of its α-subunit. We then generated a new cell line, α-ENaC-psf, that constitutively overexpresses wild-type mouse α-ENaC in γ-ENaC-TetOn-mCCD, an inducible cell line derived from $mCCD_{cl1}$ cells (18), and conditionally overexpressed wild-type mouse γ-ENaC in response to Dox in a CD principal cell line (5, 17). Figure 5*A* shows that

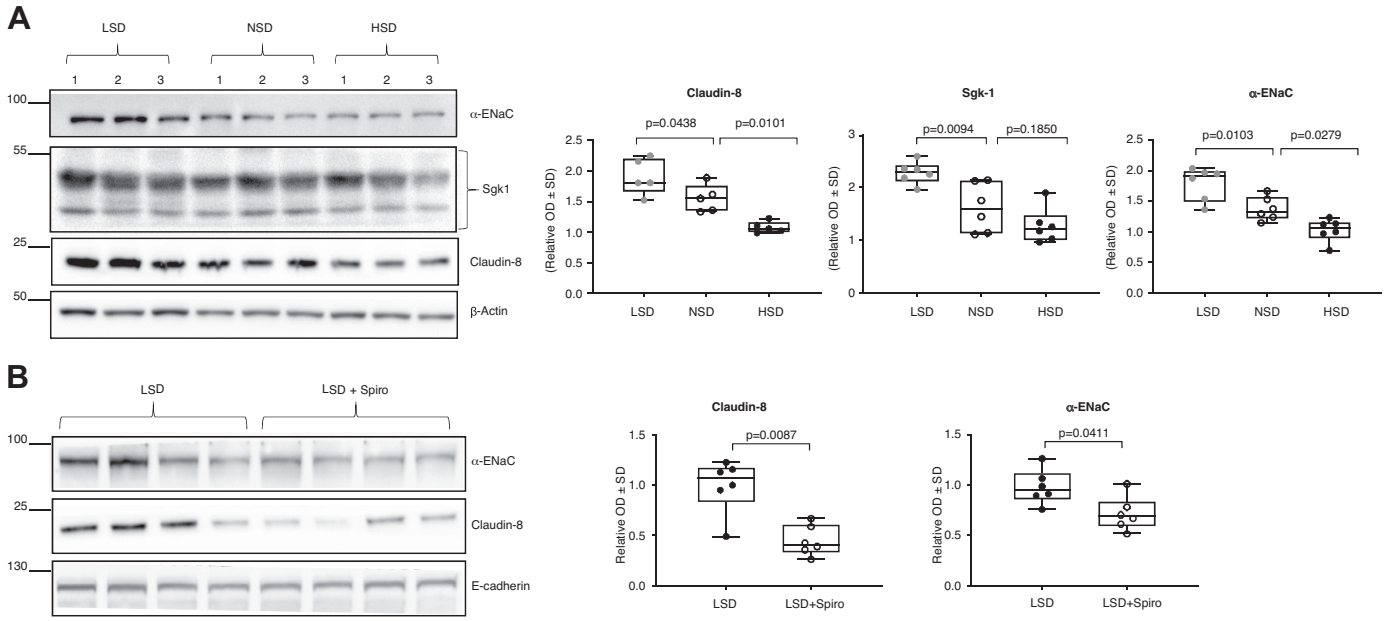

Figure 4. Aldosterone regulates claudin-8 expression in the mouse kidney. Normal mice were subjected to a low-Na^+ diet (0.01%; LSD), normal-Na^+ diet (0.18%; NSD), or high-Na^+ diet (1.25%; HSD) for 7 days. *A*, *left*: Western blot analysis showing the effect of dietary Na^+ on claudin-8, α-epithelial Na^+ channel (α-ENaC), and serum/glucocorticoid-regulated kinase 1 (Sgk-1) abundance on the kidney cortex of 3 animals for each experimental group. *Right*, relative densitometric quantification of immunoblots from the kidney cortex of 6 animals. β-Actin was used as a loading control. *B*: effect of mineralocorticoid receptor blockade on claudin-8 expression. Mice were fed an LSD (0.01%) and treated or not treated with 0.35 mg/100 g body wt/day of spironolactone (Spiro) for 1 wk before extraction of kidney cortex protein. *Left*, Western blot showing the effect of spironolactone on claudin-8 and α-ENaC protein abundance on the kidney cortex of 4 animals for each experimental group. *Right*, densitometric quantification of immunoblots from the kidney cortex of 6 animals. E-cadherin was used as a loading control. Statistical analysis was performed by one-way ANOVA. OD, optical density.

J_ID: AJPRENAL ART NO: F-00207-2021 Date: 11-October-21 12:00 Page: 7 Total Pages: 13 ini: 6//RM

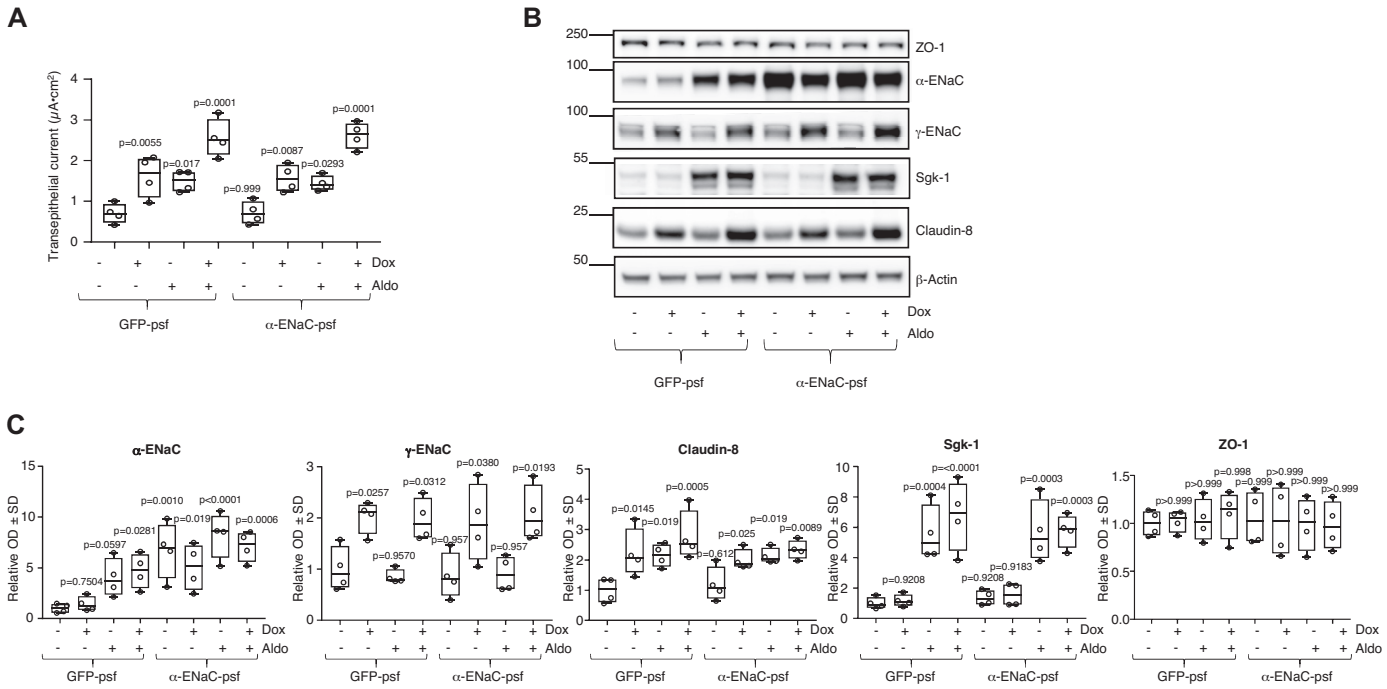

Figure 5. Epithelial Na^+ channel (ENaC) and serum/glucocorticoid-regulated kinase 1 (Sgk-1) are not involved in changes of claudin-8 expression levels in response to aldosterone (Aldo). *A*: γ-ENaC-TetOn-mCCD cells were transduced with lentiviruses encoding green fluorescence protein (GFP) or mouse α-ENaC (α-psf). Cells were treated or not treated with 10^{-6} M aldosterone for 24 h or/and 1.25 mg/mL doxycycline (Dox) for 2.5 days. *B*: representative immunoblots from 4 independent experiments showing the effect of α-ENaC and/or γ-ENaC overexpression on claudin-8, Sgk-1, and zonula occludens-1 (ZO-1) abundance. *C*: graphs depicting relative densitometric quantification of immunoblots from 4 experiments. Statistical analysis was performed by one-way ANOVA. OD, optical density.

overexpression of α-ENaC did not alter transepithelial current in both the absence and the presence of Dox-induced γ-ENaC overexpression. As expected, stimulation of transepithelial Na^+ transport by γ-ENaC overexpression increased claudin-8 abundance (5). Figure 5*A* also shows that transepithelial current induced by γ-ENaC overexpression was additive to the effect of aldosterone and that this was independent of α-ENaC overexpression. However, the effects of aldosterone and γ-ENaC overexpression on claudin-8 expression levels were not additive. Increased Sgk-1 abundance was taken as a positive control of the efficacy of aldosterone treatment. Therefore, increased claudin-8 abundance in response to aldosterone is independent of its effect on α-ENaC.

AQ: 10

We then decided to investigate the role of the classical aldosterone-induced gene Sgk-1 on claudin-8 abundance in the γ-ENaC-TetOn-mCCD cell line. Pharmacological inhibition of Sgk-1 by a specific inhibitor (GSK650394) (21) did not alter the effect of aldosterone on claudin-8 expression (Fig. 6*A*). Moreover, claudin-8 expression was not altered in the renal cortex of kidney tubule-specific Sgk-1 knockout mice (Fig. 6*B*). These results indicate that the upregulation of claudin-8 by aldosterone is most likely independent of Sgk-1.

F6

Inhibition of Aldosterone-Activated Protein Kinase Activity Prevents the Upregulation of Claudin-8 Abundance in Response to Aldosterone in Cultured Mouse CD Principal Cells

Because transcription of many genes is modulated by protein kinase pathways, we investigated whether the observed change in claudin-8 abundance is also mediated by aldosterone-activated protein kinases.

Activation of GSK3 by aldosterone has been recently reported in several studies (22–24). Figure 7 shows that inhibition of GSK3 by two structurally unrelated pharmacological inhibitors SB216763 (Fig. 7*A* and Supplemental Fig. S5) and LiCl (Fig. 7*B* and Supplemental Fig. S5) prevented the increase in claudin-8 mRNA and protein levels induced by aldosterone. Increased abundance of Sgk-1, an aldosterone-induced gene, was taken as a control of the efficacy of aldosterone treatment. Interestingly, Sgk-1 induction by aldosterone was also decreased by LiCl treatment at the protein level, and both GSK3 inhibitors decreased aldosterone-induced Sgk-1 mRNA levels. These results indicate that the GSK3 signaling pathway controls claudin-8 expression and modulates MR signaling.

F7

To further examine the aldosterone signaling pathway, we performed a functional kinase assay for the identification of phosphopeptide profiles in response to aldosterone treatment in $mCCD_{cl1}$ cells. The results of these experiments are shown in Supplemental Fig. S4 and Supplemental Tables S1 and S2. In particular, higher activities of tyrosine-protein kinases Lyn, Abl, and epidermal growth factor receptor (EGFR) as well as the serine/threonine kinase AMP-activated protein kinase (AMPK) were detected in aldosterone-treated cells. We then decided to assess the effect of these protein kinases in cultured $mCCD_{cl1}$ cells. Figure 7*C* and Supplemental Fig. S5*A* show that pharmacological inhibition of Lyn by bafetinib (25) prevented the upregulation of both claudin-8 mRNA and protein in response to aldosterone. Furthermore, the

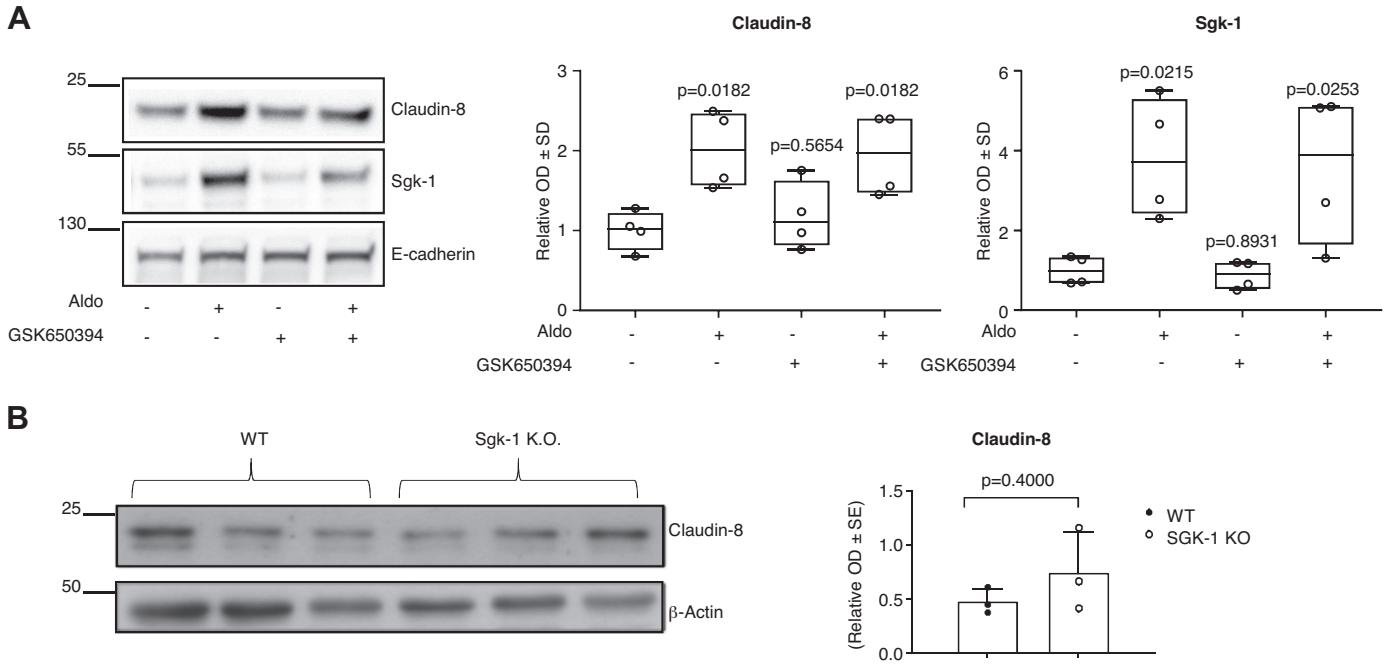

Figure 6. Serum/glucocorticoid-regulated kinase 1 (Sgk-1) is not involved in changes of claudin-8 expression levels in response to aldosterone (Aldo). *A*: γENaC-TetOn-mCCD cells were grown to confluence on filters and treated or not treated with 10^{-6} M aldosterone for 24 h, followed by treatment or no treatment for 12 h with 1 μM GSK650394, a Sgk-1 inhibitor. Representative immunoblots from 4 independent experiments showing the effect of aldosterone or/and doxycycline treatment and/or Sgk-1 inhibitor on Sgk-1 and claudin-8 abundance are shown. E-cadherin was used as a loading control. *B*, *left*: immunoblots showing the effect of kidney tubule-specific Sgk-1 deletion on claudin-8 abundance in the kidney cortex of 3 wild-type (WT) mice and 3 Sgk-1 knockout (KO) mice. β-Actin was used as a loading control. *Right*, relative densitometric quantification of immunoblots from the kidney cortex of 3 animals. Statistical analysis was performed by one-way ANOVA or a Kruskal–Wallis test when appropriate. OD, optical density.

same effect was observed by pharmacological blockade of Abl by bosutinib (26) (Fig. 7*D* and Supplemental Fig. S5*A*). Sgk-1 mRNA and protein levels were also decreased by Lyn or Abl inhibition. In contrast, neither inhibition of EGFR by AG1478 nor activation of AMPK by 5-aminoimidazole-4-carboxamide ribonucleotide altered the aldosterone-induced increase in claudin-8 expression levels (Supplemental Fig. S6).

We finally assessed whether aldosterone alters the expression levels of GSK3, Lyn, and Abl. The results shown in Supplemental Fig. S7 indicate that mRNA levels of these three protein kinases were unchanged in response to aldosterone.

Taken together, these results indicate that GSK3, Lyn, and Abl signaling pathways are involved in the regulation of claudin-8 expression by aldosterone.

DISCUSSION

Aldosterone classically directly stimulates Na^+ reabsorption and K^+ secretion by the so-called aldosterone-sensitive distal nephron, which includes the late distal convoluted tubule, connecting tubule, and CD. In the present study, we show that aldosterone increases claudin-8 expression levels. Claudin-8 is a core tight junction protein, reported to be specific and highly expressed along the aldosterone-sensitive distal nephron. Indeed, in cultured CD principal cells, aldosterone effects on transepithelial Na^+ transport are associated with parallel changes in claudin-8 expression levels. This upregulation of claudin-8 in response to aldosterone was confirmed in vivo. We showed that mice subjected to low salt intake, which increases aldosterone secretion, displayed higher claudin-8 abundance. Whereas, mice subjected to high salt intake, which decreases aldosterone secretion, exhibited lower claudin-8 expression levels. It is worth mentioning that changes in claudin-8 protein abundance were not associated with a parallel increase in claudin-8 mRNA levels. This result may indicate that in contrast with cultured cells, complex interconnected mechanisms control claudin-8 expression at the mRNA and protein levels. However, the main conclusion of our study that aldosterone upregulates claudin-8 protein levels remains valid. Our results are in agreement with the reported aldosterone-stimulated expression of claudin-8 in the distal colon (16) as well as the glucocorticoid-induced upregulation of claudin-8 in lung epithelia (27). In addition, a recent study has shown that spironolactone, an MR antagonist, prevented the increase in expression of both claudin-8 and claudin-4 in rats with early stages of diabetic nephropathy (28).

The effect of aldosterone is most likely mediated via the MR since 17-hydroxyprogesterone, an inhibitor of the MR (20), abolished its effect in cultured CD cells and spironolactone, an antagonist of the MR active in vivo, prevented the effect of an LSD in mice. Our results indicate that aldosterone most likely modulates claudin-8 expression at the transcriptional level since claudin-8 mRNA abundance was increased, actinomycin D, an inhibitor of transcription, as well as silencing of claudin-8 by shRNA abolished its effect, and in silico analysis of claudin-8 promoter revealed several MR- and GR-binding sites. The involvement of the GR in this

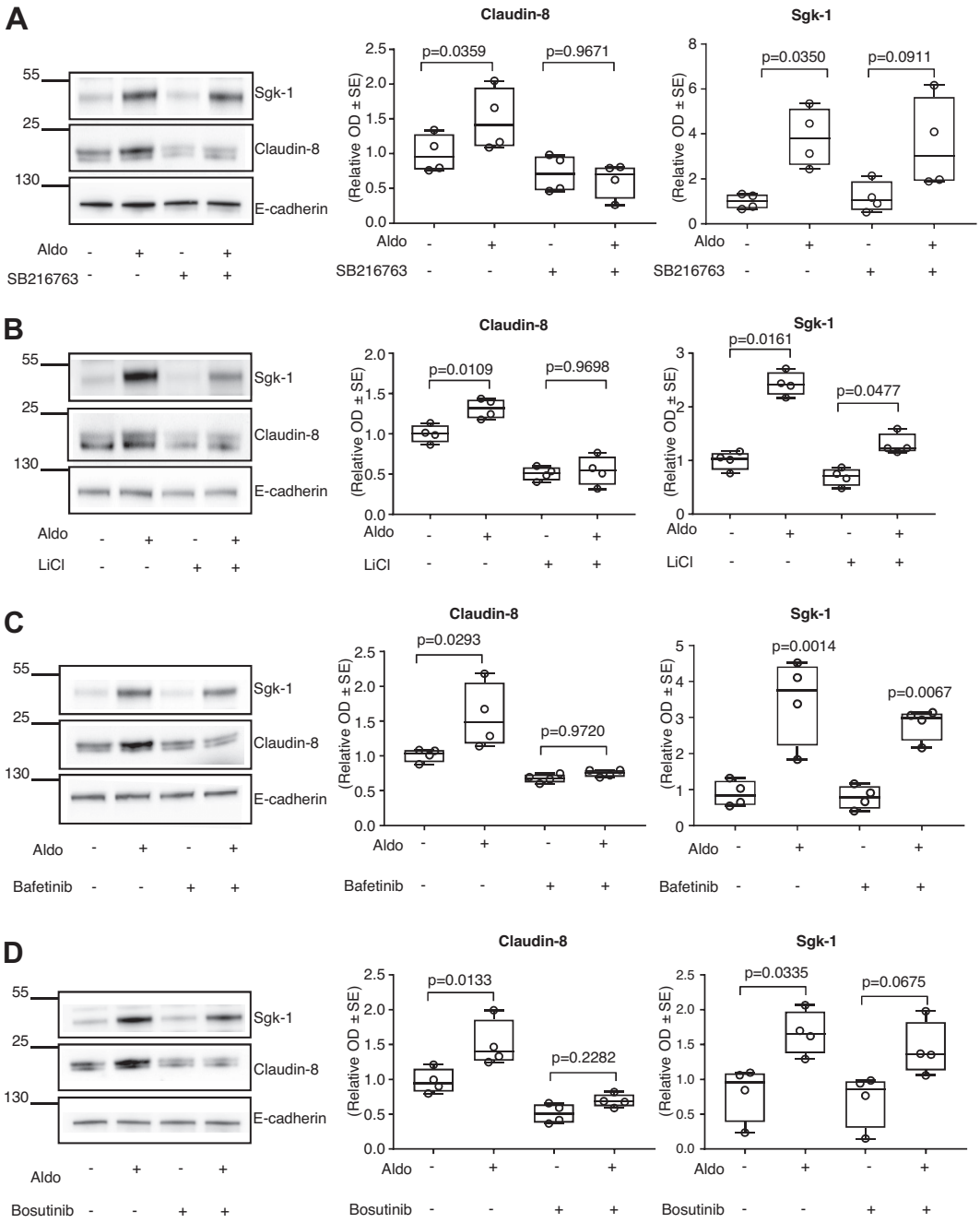

Figure 7. Functional inhibition of aldosterone (Aldo)-activated protein kinase activity prevents the upregulation of claudin-8 expression in response to aldosterone in cultured mouse collecting duct principal cells. $mCCD_{cl1}$ cells were grown to confluence on filters and treated or not treated with 10^{-6} M aldosterone for 24 h, followed by treatment or no treatment with 10 μM SB216763 (*A*) or 20 mM LiCl (*B*), two glycogen synthase kinase-3 inhibitors, 10 μM bafetinib (*C*), a Lyn inhibitor, or 10 μM bosutinib (*D*), an Abl inhibitor. *A*, *left*: representative immunoblots showing the effect of aldosterone and/or SB216763 treatment on claudin-8 and serum/glucocorticoid-regulated kinase 1 (Sgk-1) expression. *Right*, bar graphs depicting relative densitometric quantification of immunoblots from 4 experiments. *B*, *left*: representative immunoblots showing the effect of aldosterone and/or LiCl treatment on claudin-8 and Sgk-1 expression. *Right*, bar graphs depicting relative densitometric quantification of immunoblots from 4 experiments. *C*, *left*: representative immunoblots showing the effect of aldosterone and/or bafetinib treatment on claudin-8 and Sgk-1 expression. *Right*, bar graphs depicting relative densitometric quantification of immunoblots from 4 experiments. *D*, *left*: representative immunoblots showing the effect of aldosterone and/or bosutinib treatment on claudin-8 and Sgk-1 expression. *Right*, bar graphs depicting relative densitometric quantification of immunoblots from 4 experiments. Expression of E-cadherin was used as a loading control. Results are means ± SD from 4 independent experiments. Statistical analysis was performed by one-way ANOVA. OD, optical density.

observed effect of aldosterone cannot be excluded since the MR and the GR share most of their signaling pathways and mechanisms of action leading to the induction or repression of a large number of common target genes, including Sgk-1. Our results also showed that the effect of aldosterone is independent of ENaC α-subunit expression level and transepithelial Na^+ transport. Indeed, α-ENaC overexpression did not alter claudin-8 expression.

AQ: 11

Our previous work showed that claudin-8 is highly implicated in the generation of an Na^+ barrier in mCCD cells (5). The association between increased claudin-8 expression levels and a more efficient Na^+ diffusion barrier was also demonstrated in response to aldosterone in the distal colon (16). However, claudin-8 in association with claudin-4 was shown to generate Cl^- permeability (4), and claudin-8 knockout is associated with NaCl wasting (29). It is, therefore, reasonable to speculate that increased claudin-8 expression levels and lateral membrane localization in response to aldosterone are aimed at preventing luminal backflux of reabsorbed Na^+ as well as reinforcing the paracellular Cl^- reabsorption pathway. Indeed, it is especially important to prevent luminal backflux of reabsorbed Na^+ in aldosterone-responsive epithelia such as the aldosterone-sensitive distal nephron and distal colon. In these epithelia, a steep Na^+ concentration gradient from the interstitium to the lumen is present, which is further increased upon aldosterone stimulation. This effect might be especially important in the kidney medulla where the interstitium-to-lumen Na^+ gradient is very large.

In this study, we found that aldosterone did not alter transepithelial resistance in $mCCD_{cl1}$ cells. Transepithelial resistance was expected to rise when claudin-8 abundance was increased, as demonstrated in our previous work (5). The absence of a large variation of transepithelial resistance in response to benzamil indicates that ENaC minimally contributes to transepithelial resistance. Therefore, ENaC stimulation by aldosterone does not explain the absence of increased transepithelial resistance despite increased expression levels and membrane localization of claudin-8 (5). Alternatively, aldosterone may modulate the expression levels of several claudin species with opposite effects on electrical resistance. For example, a change in claudin combination leading to increased barrier to cations together with increased permeability to anions may result in the absence of a significant variation of transepithelial resistance. Alternatively, aldosterone may act as a "priming" stimulus by increasing membrane claudin-8, and a second "activating" stimulus, such as increased γ-ENaC abundance, might be required to incorporate claudin-8 to the tight junctional complex and to increase paracellular resistance.

Because a phosphorylation process has been reported to be implicated in the control of tight junction components (30), we investigated the role of protein kinases in the aldosterone effect. We showed that GSK3, Lyn, and Abl signaling pathways are most likely involved in the aldosterone stimulation of claudin-8 expression. Several pieces of experimental evidence suggested that activation of several protein kinase families by aldosterone, such as MAPK, PKC, ERK1/2, and PKD, occurs through transactivation of EGFR (31–34). This transactivation of EGFR is most likely mediated by activation of the cytosolic tyrosine kinase c-Src (35). Our results are in agreement with these findings since tyrosine protein kinases Lyn and Fyn are members of the Src family, and Pyk2 forms active multi-subunit signaling complexes with Src family members that directly phosphorylate EGFR (36, 37). Although higher activity of EGFR was detected by analysis of phosphopeptide profiles in aldosterone-treated $mCCD_{cl1}$ cells (Supplemental Fig. S4), pharmacological inhibition of EGFR (38) did not alter the effect of aldosterone on claudin-8 expression (Supplemental Fig. S6). Therefore, increased claudin-8 abundance does not rely on EGFR transactivation. However, tyrosine kinases such as Fyn and Pyk2 have been implicated in the phosphorylation and activation of GSK3 in mammalian cells (39, 40). These observations fit with our results showing that increased claudin-8 expression is dependent on GSK3 activity. Our results also showed that induction of Sgk-1 in response to aldosterone was reduced after Lyn, Abl, or GSK3 inhibition. These observations argue for a permissive or potentiating effect of these signaling pathways on the transcriptional activity of the MR.

Perspectives and Significance

In summary, our results demonstrated that in addition to stimulation of Na^+ transport by the CD via ENaC, aldosterone also modulates the composition of the tight junctional complex through the upregulation of claudin-8. This study also reveals and confirms that composition of the junctional complex can be regulated in response to physiological stimuli involving multiple protein kinases.

SUPPLEMENTAL DATA

Supplemental Tables S1 and S2 and Supplemental Figs. S1–S7: https://doi.org/10.6084/m9.figshare.16652182.v1.

ACKNOWLEDGMENTS

We thank Prof. Johannes Loffing (Institute of Anatomy, University of Zürich) for kindly providing the α-ENaC subunit antibody.

GRANTS

This work was supported by the National Center of Competence in Research Kidney Control of Homeostasis and Swiss National Science Foundation Grant Nos. 31003 A_156736/1 and 31003 A_175471/1 to E.F.

DISCLOSURES

No conflicts of interest, financial or otherwise, are declared by the authors.

AUTHOR CONTRIBUTIONS

A.S., Y.W., and E.F. conceived and designed research; A.S., Y.W., A.C., V.O., K.U., and E.F. performed experiments; A.S., Y.W., A.C., I.R., S.R., V.O., O.S., and E.F. analyzed data; A.S., Y.W., A.C., I.R., and E.F. interpreted results of experiments; A.S., Y.W., I.R., and V.O. prepared figures; A.S., Y.W., and E.F. drafted manuscript; A.S., Y.W., A.C., S.R., V.O., O.S., and E.F. edited and revised manuscript; A.S., Y.W., A.C., I.R., S.R., V.O., O.S., K.U., and E.F. approved final version of manuscript.

REFERENCES

1. **Yu ASL.** Claudins and the kidney. *J Am Soc Nephrol* 26: 11–19, 2015. doi:10.1681/ASN.2014030284.
2. **Li WY**, **Huey CL**, **Yu ASL.** Expression of claudin-7 and -8 along the mouse nephron. *Am J Physiol Renal Physiol* 286: F1063–F1071, 2004. doi:10.1152/ajprenal.00384.2003.
3. **Hou J**, **Rajagopal M**, **Yu ASL.** Claudins and the kidney. *Annu Rev Physiol* 75: 479–501, 2013. doi:10.1146/annurev-physiol-030212-183705.

4. **Hou J**, **Renigunta A**, **Yang J**, **Waldegger S.** Claudin-4 forms paracellular chloride channel in the kidney and requires claudin-8 for tight junction localization. *Proc Natl Acad Sci USA* 107: 18010–18015, 2010. doi:10.1073/pnas.1009399107.
5. **Sassi A**, **Wang Y**, **Chassot A**, **Komarynets O**, **Roth I**, **Olivier V**, **Crambert G**, **Dizin E**, **Boscardin E**, **Hummler E**, **Feraille E.** Interaction between epithelial sodium channel γ-subunit and claudin-8 modulates paracellular sodium permeability in renal collecting duct. *J Am Soc Nephrol* 31: 1009–1023, 2020. doi:10.1681/ASN.2019080790.
6. **Pascual-Le Tallec L**, **Lombès M.** The mineralocorticoid receptor: a journey exploring its diversity and specificity of action. *Mol Endocrinol* 19: 2211–2221, 2005. doi:10.1210/me.2005-0089.
7. **Chen SY**, **Bhargava A**, **Mastroberardino L**, **Meijer OC**, **Wang J**, **Buse P**, **Firestone GL**, **Verrey F**, **Pearce D.** Epithelial sodium channel regulated by aldosterone-induced protein sgk. *Proc Natl Acad Sci USA* 96: 2514–2519, 1999. doi:10.1073/pnas.96.5.2514.
8. **Soundararajan R**, **Zhang TT**, **Wang J**, **Vandewalle A**, **Pearce D.** A novel role for glucocorticoid-induced leucine zipper protein in epithelial sodium channel-mediated sodium transport. *J Biol Chem* 280: 39970–39981, 2005. doi:10.1074/jbc.M508658200.
9. **Bhalla V**, **Soundararajan R**, **Pao AC**, **Li H**, **Pearce D.** Disinhibitory pathways for control of sodium transport: regulation of ENaC by SGK1 and GILZ. *Am J Physiol Renal Physiol* 291: F714–F721, 2006. doi:10.1152/ajprenal.00061.2006.
10. **Summa V**, **Mordasini D**, **Roger F**, **Bens M**, **Martin P-Y**, **Vandewalle A**, **Verrey F**, **Féraille E.** Short term effect of aldosterone on Na,K-ATPase cell surface expression in kidney collecting duct cells. *J Biol Chem* 276: 47087–47093, 2001. doi:10.1074/jbc.M107165200.
11. **Ferrari P**, **Krozowski Z.** Role of the 11beta-hydroxysteroid dehydrogenase type 2 in blood pressure regulation. *Kidney Int* 57: 1374–1381, 2000. doi:10.1046/j.1523-1755.2000.00978.x.
12. **Frindt G**, **Silver RB**, **Windhager EE**, **Palmer LG.** Feedback regulation of Na channels in rat CCT. III. Response to cAMP. *Am J Physiol Renal Physiol* 268: F480–F489, 1995. doi:10.1152/ajprenal.1995.268.3.F480.
13. **Fodstad H**, **Gonzalez-Rodriguez E**, **Bron S**, **Gaeggeler H**, **Guisan B**, **Rossier BC**, **Horisberger J-D.** Effects of mineralocorticoid and K^+ concentration on K^+ secretion and ROMK channel expression in a mouse cortical collecting duct cell line. *Am J Physiol Renal Physiol* 296: F966–F975, 2009. doi:10.1152/ajprenal.90475.2008.
14. **Mamenko M**, **Zaika O**, **Prieto MC**, **Jensen VB**, **Doris PA**, **Navar LG**, **Pochynyuk O.** Chronic angiotensin II infusion drives extensive aldosterone-independent epithelial Na^+ channel activation. *Hypertension* 62: 1111–1122, 2013. doi:10.1161/HYPERTENSIONAHA.113.01797.
15. **Morla L**, **Doucet A**, **Lamouroux C**, **Crambert G**, **Edwards A.** The renal cortical collecting duct: a secreting epithelium? *J Physiol* 594: 5991–6008, 2016. doi:10.1113/JP272877.
16. **Amasheh S**, **Milatz S**, **Krug SM**, **Bergs M**, **Amasheh M**, **Schulzke J-D**, **Fromm M.** Na^+ absorption defends from paracellular back-leakage by claudin-8 upregulation. *Biochem Biophys Res Commun* 378: 45–50, 2009. doi:10.1016/j.bbrc.2008.10.164.
17. **Wang Y-B**, **Leroy V**, **Maunsbach AB**, **Doucet A**, **Hasler U**, **Dizin E**, **Ernandez T**, **de Seigneux S**, **Martin P-Y**, **Féraille E.** Sodium transport is modulated by p38 kinase-dependent cross-talk between ENaC and Na,K-ATPase in collecting duct principal cells. *J Am Soc Nephrol* 25: 250–259, 2014. doi:10.1681/ASN.2013040429.
18. **Gaeggeler H-P**, **Gonzalez-Rodriguez E**, **Jaeger NF**, **Loffing-Cueni D**, **Norregaard R**, **Loffing J**, **Horisberger J-D**, **Rossier BC.** Mineralocorticoid versus glucocorticoid receptor occupancy mediating aldosterone-stimulated sodium transport in a novel renal cell line. *J Am Soc Nephrol* 16: 878–891, 2005. doi:10.1681/ASN.2004121110.
19. **Faresse N**, **Lagnaz D**, **Debonneville A**, **Ismailji A**, **Maillard M**, **Fejes-Toth G**, **Náray-Fejes-Tóth A**, **Staub O.** Inducible kidney-specific Sgk1 knockout mice show a salt-losing phenotype. *Am J Physiol Renal Physiol* 302: F977–F985, 2012. doi:10.1152/ajprenal.00535.2011.
20. **Rafestin-Oblin M-E**, **Fagart J**, **Souque A**, **Seguin C**, **Bens M**, **Vandewalle A.** 11β-Hydroxyprogesterone acts as a mineralocorticoid agonist in stimulating Na^+ Absorption in mammalian principal cortical collecting duct cells. *Mol Pharmacol* 62: 1306–1313, 2002. doi:10.1124/mol.62.6.1306.
21. **Sherk AB**, **Frigo DE**, **Schnackenberg CG**, **Bray JD**, **Laping NJ**, **Trizna W**, **Hammond M**, **Patterson JR**, **Thompson SK**, **Kazmin D**, **Norris JD**, **McDonnell DP.** Development of a small molecule serum and glucocorticoid-regulated kinase 1 antagonist and its evaluation as a prostate cancer therapeutic. *Cancer Res* 68: 7475–7483, 2008. doi:10.1158/0008-5472.CAN-08-1047.
22. **Brem AS**, **Gong R.** Therapeutic targeting of aldosterone: a novel approach to the treatment of glomerular disease. *Clin Sci (Lond)* 128: 527–535, 2015. doi:10.1042/CS20140432.
23. **Zhang Y-D**, **Ding X-J**, **Dai H-Y**, **Peng W-S**, **Guo N-F**, **Zhang Y**, **Zhou Q-L**, **Chen X-L.** SB-216763, a GSK-3β inhibitor, protects against aldosterone-induced cardiac, and renal injury by activating autophagy. *J Cell Biochem* 119: 5934–5943, 2018. doi:10.1002/jcb.26788.
24. **Schmidt-Ott KM**, **Barasch J.** WNT/beta-catenin signaling in nephron progenitors and their epithelial progeny. *Kidney Int* 74: 1004–1008, 2008. doi:10.1038/ki.2008.322.
25. **Santos FPS**, **Kantarjian H**, **Cortes J**, **Quintas-Cardama A.** Bafetinib, a dual Bcr-Abl/Lyn tyrosine kinase inhibitor for the potential treatment of leukemia. *Curr Opin Investig Drugs* 11: 1450–1465, 2010.
26. **Bieerkehazhi S**, **Chen Z**, **Zhao Y**, **Yu Y**, **Zhang H**, **Vasudevan SA**, **Woodfield SE**, **Tao L**, **Yi JS**, **Muscal JA**, **Pang JC**, **Guan S**, **Zhang H**, **Nuchtern JG**, **Li H**, **Li H**, **Yang J.** Novel Src/Abl tyrosine kinase inhibitor bosutinib suppresses neuroblastoma growth via inhibiting Src/Abl signaling. *Oncotarget* 8: 1469–1480, 2017. doi:10.18632/oncotarget.13643.
27. **Kielgast F**, **Schmidt H**, **Braubach P**, **Winkelmann VE**, **Thompson KE**, **Frick M**, **Dietl P**, **Wittekindt OH.** Glucocorticoids regulate tight junction permeability of lung epithelia by modulating claudin 8. *Am J Respir Cell Mol Biol* 54: 707–717, 2016. doi:10.1165/rcmb.2015-0071OC.
28. **Molina-Jijón E**, **Rodríguez-Muñoz R**, **González-Ramírez R**, **Namorado-Tónix C**, **Pedraza-Chaverri J**, **Reyes JL.** Aldosterone signaling regulates the over-expression of claudin-4 and -8 at the distal nephron from type 1 diabetic rats. *PloS One* 12: e0177362, 2017. doi:10.1371/journal.pone.0177362.
29. **Gong Y**, **Wang J**, **Yang J**, **Gonzales E**, **Perez R**, **Hou J.** KLHL3 regulates paracellular chloride transport in the kidney by ubiquitination of claudin-8. *Proc Natl Acad Sci USA* 112: 4340–4345, 2015. doi:10.1073/pnas.1421441112.
30. **González-Mariscal L**, **Tapia R**, **Chamorro D.** Crosstalk of tight junction components with signaling pathways. *Biochim Biophys Acta* 1778: 729–756, 2008. doi:10.1016/j.bbamem.2007.08.018.
31. **McEneaney V**, **Harvey BJ**, **Thomas W.** Aldosterone rapidly activates protein kinase D via a mineralocorticoid receptor/EGFR trans-activation pathway in the M1 kidney CCD cell line. *J Steroid Biochem Mol Biol* 107: 180–190, 2007. doi:10.1016/j.jsbmb.2007.03.043.
32. **Grossmann C**, **Gekle M.** Non-classical actions of the mineralocorticoid receptor: misuse of EGF receptors? *Mol Cell Endocrinol* 277: 6–12, 2007. doi:10.1016/j.mce.2007.07.001.
33. **Thomas W**, **Harvey BJ.** Mechanisms underlying rapid aldosterone effects in the kidney. *Annu Rev Physiol* 73: 335–357, 2011. doi:10.1146/annurev-physiol-012110-142222.
34. **Harvey BJ**, **Thomas W.** Aldosterone-induced protein kinase signalling and the control of electrolyte balance. *Steroids* 133: 67–74, 2018. doi:10.1016/j.steroids.2017.10.009.
35. **Braun S**, **Lösel R**, **Wehling M**, **Boldyreff B.** Aldosterone rapidly activates Src kinase in M-1 cells involving the mineralocorticoid receptor and HSP84. *FEBS Lett* 570: 69–72, 2004. doi:10.1016/j.febslet.2004.06.031.
36. **Andreev J**, **Galisteo ML**, **Kranenburg O**, **Logan SK**, **Chiu ES**, **Okigaki M**, **Cary LA**, **Moolenaar WH**, **Schlessinger J.** Src and Pyk2 mediate G-protein-coupled receptor activation of epidermal growth factor receptor (EGFR) but are not required for coupling to the mitogen-activated protein (MAP) kinase signaling cascade. *J Biol Chem* 276: 20130–20135, 2001. doi:10.1074/jbc.M102307200.
37. **Roelle S**, **Grosse R**, **Buech T**, **Chubanov V**, **Gudermann T.** Essential role of Pyk2 and Src kinase activation in neuropeptide-induced proliferation of small cell lung cancer cells. *Oncogene* 27: 1737–1748, 2008. doi:10.1038/sj.onc.1210819.
38. **Zhu XF**, **Liu ZC**, **Xie BF**, **Li ZM**, **Feng GK**, **Yang D**, **Zeng YX.** EGFR tyrosine kinase inhibitor AG1478 inhibits cell proliferation and arrests cell cycle in nasopharyngeal carcinoma cells. *Cancer Lett* 169: 27–32, 2001. doi:10.1016/s0304-3835(01)00547-x.
39. **Lesort M**, **Jope RS**, **Johnson GV.** Insulin transiently increases tau phosphorylation: involvement of glycogen synthase kinase-3β and Fyn tyrosine kinase. *J Neurochem* 72: 576–584, 1999. doi:10.1046/j.1471-4159.1999.0720576.x. AQ: 17
40. **Sayas CL**, **Ariaens A**, **Ponsioen B**, **Moolenaar WH.** GSK-3 is activated by the tyrosine kinase Pyk2 during LPA1-mediated neurite retraction. *Mol Biol Cell* 17: 1834–1844, 2006. doi:10.1091/mbc.E05-07-0688.

AUTHOR QUERIES

AUTHOR PLEASE ANSWER ALL QUERIES 1

AQau— Please confirm the given-names and surnames are identified properly by the colors. ■= Given-Name, ■= Surname

AQ1— Please read entire proof (including query page), answer queries and mark corrections (using Adobe tools per online instruction), and return it within 2 business days to the online proof review site (link provided in email). IMPORTANT: Make sure query page is included. Please only make changes that are essential to correct data errors. Requests for cosmetic and other nonessential changes to figures and text at this stage will not be accommodated.

AQ2— Please check all figures, tables, equations, and legends carefully. Changes will be made only to correct scientifically relevant errors. Please confirm or correct abbreviation definitions that have been inserted in the legends by the copy editor. If changes are required to the figures themselves, please list ALL changes requested (even if you provide a new figure).

AQ3— Please note that your manuscript has been copyedited and that style changes have been made, including those related to punctuation, abbreviations, italics, hyphens and word divisions, units of measurement, etc., to conform to Journal style preferences. Please check that no errors in meaning were inadvertently introduced. Not all of the changes are pointed out in the Author Query list, so please check all text carefully.

AQ4— Please carefully review the hierarchy of headings throughout your article.

AQ5— Please verify the affiliation details for accuracy and revise, if needed.

AQ6— Please verify accuracy of your e-mail for correspondence. (Note: this material is listed as a footnote at bottom of left column of text on the first page .)

AQ7— We note that gene and protein nomenclature is used in this manuscript. If appropriate, please define at first use and ensure that genes are italicized and proteins are not. Also verify if capitalization is correct for genes/proteins. Mark each instance where a change is needed.

AQ8— Please define "GILZ, PKD and mCCD" at first use unless these are standard abbreviations in your field.

AQ9— Please check any ORCID links and/or URLs in your manuscripts to ensure they link to the intended materials.

AQ10— Please check the sentence "Therefore, increased claudin-8 abundance in response. . ." for clarity.

AQ11— Please check the sentence "The involvement of the GR in this observed effect of . . ." for clarity.

AQ12— Please check if the edits made to the sentence "The association between increased claudin-8. . ." is correct.

AQ13— Please verify that all supplemental DOI links are public and active and access all intended supplemental material.

AQ14— Please verify that any GRANTS are listed correctly.

AUTHOR QUERIES

AUTHOR PLEASE ANSWER ALL QUERIES 2

AQ15— The text in the DISCLOSURES section reflects your data entry into the Peer Review submission. Is this still complete, relevant, and accurate?

AQ16— The text in the AUTHOR CONTRIBUTIONS section reflects your data entry into the Peer Review submission. Is this still complete and accurate? If changes are needed, please follow this template.

AQ17— Please verify the revised Ref. 39.

AQ18— Please define "EGR and ATG" in Fig. 3 legend, unless these are standard definitions in your field.